Research Article

Increased caveolin 1 by human antigen R exacerbates *Porphyromonas gingivali*-induced atherosclerosis by modulating oxidative stress and inflammatory responses

Fang Miao, MM[1], Yangyang Lei, BS[2], Yunfei Guo, BS[1], Yongxia Ma, MM[2], Ye Zhang, BS[1], Binbin Jia, BS[2]

[1]Department of Prevention and Healthcare, Lanzhou Stomatology Hospital, Lanzhou, [2]Department of Cardiology, The Second People's Hospital of Lanzhou City, Lanzhou, China.

*Corresponding author:
Binbin Jia,
Department of Cardiology, The Second People's Hospital of Lanzhou City, Lanzhou, China.

jbb13919319334@163.com

ABSTRACT

Objective: Many different types of infectious oral diseases have been identified clinically, including chronic periodontitis. *Porphyromonas gingivalis* is the main pathogen causing chronic periodontitis, which is closely related to atherosclerosis (AS) and can promote the expression levels of caveolin 1 (Cav-1) and induced ribonucleic acid (RNA)-binding protein human antigen R (HuR). However, the roles of Cav-1 and its relationship with HuR in *P. gingivalis*-mediated AS progression remain largely unknown. Here, we aimed to detect the role and molecular mechanisms of Cav-1 in *P. gingivalis*-mediated AS.

Material and Methods: To investigate the role of Cav-1 in *P. gingivalis*-mediated AS, we infected human umbilical vein endothelial cells (HUVECs) with *P. gingivalis* at a multiplicity of infection of 100:1 for 6, 12, and 24 h to simulate *P. gingivalis*-induced AS models *in vitro* and then transfected them with Cav-1 small interfering RNA to silence Cav-1. Combining molecular biology experimental techniques such as cell counting kit-8 assay, enzyme-linked immunosorbent assay, immunofluorescence staining, flow cytometry, Western blotting, and Oil Red O staining, and apolipoprotein E-deficient AS model mice, the impacts of Cav-1 on cell viability, inflammation, oxidative stress, apoptosis, Cav-1 and intercellular cell adhesion molecule-1 (ICAM-1) levels, and atherosclerotic plaque formation were investigated. Then, the relationship between Cav-1 and HuR was investigated through biotin pull-down and RNA immunoprecipitation assays, reverse transcription quantitative polymerase chain reaction, and Western blot.

Results: *P. gingivalis* can induce Cav-1 expression in a time- and dose-dependent manner ($P < 0.05$). This effect can inhibit the proliferation of HUVECs ($P < 0.05$). Cav-1 interference repressed inflammatory response, reactive oxygen species (ROS) and ICAM-1 levels, and apoptosis in the HUVECs ($P < 0.05$). Cav-1 messenger RNA was stabilized by HuR, which can bind to the 3' untranslated region of Cav-1. Increase in HuR level reversed the effects of Cav-1 silencing on ROS and ICAM-1 levels and apoptosis in the HUVECs ($P < 0.05$). In addition, the levels of inflammatory response, oxidative stress, and atherosclerotic plaque formation induced by *P. gingivalis* in the mouse model were significantly reduced after Cav-1 expression was inhibited ($P < 0.05$).

Conclusion: HuR-activated Cav-1 may promote atherosclerotic plaque formation by modulating inflammatory response and oxidative stress, leading to AS.

Keywords: Caveolin 1, *Porphyromonas gingivalis*, Atherosclerosis, Inflammation

INTRODUCTION

Clinical staff often encounters patients with chronic infectious diseases, such as periodontitis. These diseases not only damage periodontal tissues but also exert considerable effects on many systemic diseases, including rheumatoid arthritis.[1,2] From the perspective of clinical epidemiology, periodontitis may be a risk factor for atherosclerosis (AS).[3,4] *Porphyromonas gingivalis* is the main pathogen causing chronic periodontitis, which is closely related to AS. The presence of *P. gingivalis* antibodies in the sera and *P. gingivalis* deoxyribonucleic acid (DNA) in the plaques of patients with AS has been demonstrated.[5-7] *P. gingivalis* can survive in macrophages and can be transferred between cells and peripheral organs.[8-10] Chronic *P. gingivalis* infection in periodontal tissues increases the expression of interleukin (IL)-6 and the matrix metalloproteinase family in the plasma, leading to a systemic inflammatory response. This state can affect endothelial cells, causing them to be in an activated state, and the altered functions of the cells lead to AS.[11] Therefore, studying and analyzing the relationship between AS and *P. gingivalis*, and their mechanisms and pathways of action are extremely important.

The caveolin 1 (Cav-1) gene is located on human chromosome 7q31.2 and encodes a 22 kda Cav-1 protein that has a scaffolding function and is the main component of the concave structure on the cell membrane surface.[12] Cav-1 can be found in terminally differentiated cells, such as adipocytes and endothelial cells, and participates in the regulation of cell signaling pathways by recognizing specific sequences and binding to various signaling molecules, playing an important regulatory role in various cellular physiological processes. Cav-1 knockdown can lead to cancer, diabetes, and Alzheimer's disease.[13-15] It can affect endothelial cells and promote the expression of inflammatory factors in cells, thus facilitating the formation of plaque and development of AS. In addition, after oral infection with *P. gingivalis*, a large amount of Cav-1, which is essential for internalization, accumulates in oral epithelial cells.[16] However, whether Cav-1 promotes AS in individuals with *P. gingivalis* infection which remains unclear.

Human antigen R (HuR), as one of the earliest discovered ribonucleic acid (RNA)-binding proteins, can regulate the expression of various genes, such as vascular endothelial growth factor, p21, and IL-6 genes, by stabilizing target protein messenger RNA (mRNA). By regulating these functional proteins, HuR participates in a variety of processes, such as cell division, tumorigenesis, and inflammatory response. Adenylate uridine–rich elements (AREs) in the 3′ untranslated regions (UTRs) of most HuR proteins target mRNAs, but HuR can specifically bind to the ARE elements in the 5′ UTRs of some target mRNAs.[17] Moreover, HuR can regulate the protein expression of Cav-1 through post-transcriptional regulation.[18] However, whether HuR acts as an RNA-binding protein to enhance Cav-1 translation during the *P. gingivalis*-mediated pathogenesis of AS remains unclear.

In this study, we investigated and analyzed the role of Cav-1 on inflammation and apoptosis and its underlying mechanisms after infection of human umbilical vein endothelial cells (HUVECs) by *P. gingivalis*. The results suggested that *P. gingivalis* infection promotes AS development and causes different diseases, providing a reference for related research.

MATERIAL AND METHODS

Establishment of *P. gingivalis*-induced atherosclerotic mouse model

This study was approved by the Animal Experiment Ethics Committee of the Second People's Hospital of Lanzhou (LZSKQYY-LL-ZD-2024-01). A total of 15 apolipoprotein E-deficient (ApoE$^{-/-}$) mice (males, 6 weeks old, 20–22 g) were purchased from the medical experimental center of Lanzhou University. The mice were kept in a standard environment with controlled temperature (21–23°C) and humidity (60% ± 5%) under specific pathogen-free conditions in individually ventilated cages. They had access to food and water ad libitum. To study and analyze the relationship between AS formation and *P. gingivalis* infection, we randomly divided ApoE$^{-/-}$ mice into three groups: ApoE$^{-/-}$ group, ApoE$^{-/-}$ + *P. gingivalis* + si-NC group, and ApoE$^{-/-}$ + *P. gingivalis* + si-Cav-1 group (*n* = 5). The ApoE$^{-/-}$ mice were injected with *P. gingivalis* (10^7 colony-forming unit in 0.1 mL of phosphate buffered saline [PBS]) through the tail vein once a week.[19] The small interfering RNA (siRNA) sequences transfected into the mice were as follows: CCACCTTCACTGTGACGAAAT (si-Cav-1) and TTCTCCGAACGTGTCACGT (si-NC). siRNA (100 μg) was injected into the ApoE$^{-/-}$ mice through the tail vein every 3 days 5 times (20 μg/injection). After 16 weeks, the mice were exposed to isoflurane (1.5–2%; 26675-46-7, Yaji Biological, Shanghai, China) and then euthanized through cervical dislocation,[20] and blood and aorta samples were collected. Blood collected from the orbital vascular plexus was centrifuged at 3000×g for 8 min to obtain the serum. Finally, the blood and aorta were stored at −80°C for experiments.

Cell culture and transfection

P. gingivalis strain American type culture collection 33277 and HUVECs were obtained from the American Tissue Culture Collection (33277, Manassas, VA, USA) and ScienCell Research Laboratories (8000, Carlsbad, CA, USA), respectively. HUVECs were authenticated by examining short tandem repeat profiling, cell morphology and growth characteristics, and detected mycoplasma contamination

using the Mycoplasma polymerase chain reaction (PCR) Detection Kit Mycoplasma Detection Kit (iCell-MD01-001, iCell Bioscience Inc, Shanghai, China). An endothelial cell (ScienCell, Carlsbad, CA, USA) medium containing 1% endothelial cell growth supplement (1052, ScienCell, Carlsbad, CA, USA), 1% penicillin/streptomycin (ST488S, Beyotime, Shanghai, China), and 5% fetal bovine serum (C0235, Beyotime, Shanghai, China) was prepared, and the HUVECs were seeded into the medium. The medium was then placed in a carbon dioxide (CO_2) incubator. The cells were observed, and when the density was at least 80%, the cells were digested with trypsin (P4201, Beyotime, Shanghai, China). Passage manipulation was then performed on the cells. The HUVECs were stimulated with *P. gingivalis* (multiplicity of infection [MOI]: 25, 50, and 100) for 24 h or with *P. gingivalis* (MOI: 100) for 6, 12, and 24 h. Non-targeted control siRNA (si-NC: 5′-UUC UCC GAA CGU GUC ACG UTT-3′), specific siRNA against Cav-1 (si-Cav-1: 5′-CCC ACU CUU UGA AGC UGU UTT-3′), HuR (si-HuR: 5′-UUC AUC GUC CUG UGU CGA ACC-3′), and pcDNA3.1-HuR were synthesized by Shanghai Sangon Biotech Co., Ltd. Lipofectamine 3000 (10 μL; lipo3000, Thermo Fisher, Waltham, MA, USA) or si-Cav-1 or si-NC (100 nM, 10 μL) was, respectively, added in OPTI-MEM (250 μL) and stood alone at room temperature for 5 min, followed by mixed incubation for 20 min to obtain liposome transfection complex. When the confluence of the HUVECs reached 70–80%, the complexes were transferred to a six-well culture plate and incubated at 37°C in 5% CO_2 for 48 h. The knockdown efficiency was then assessed through Western blot.

RNA stability and reverse transcription quantitative PCR (RT-qPCR)

The HUVECs were treated with actinomycin D (5 μg/mL; 50–76–0, Sigma-Aldrich, St. Louis, Missouri, USA) for 0, 2, and 4 h and then incubated with TRIzol reagent (15596–026; Thermo Fisher, Waltham, MA, USA). RNA was extracted, and the remaining mRNA was analyzed through RT-qPCR.

Total RNA was extracted from the cells with TRIzol reagent and then reverse transcribed to produce complementary DNA, which was used as a template for subsequent quantitative PCR (qPCR). A qPCR machine (PIKOREAL96; Thermo Fisher, Waltham, MA, USA) and SYBR Premix EX TaqTM kits (DRR820A, TakaRa, Japan) were used. The cycle threshold value was determined, and then, the $2^{-\Delta\Delta Ct}$ method was used in calculating the Cav-1 level. The following primers pairs were used: Cav-1: 5′-GCG ACC CTA AAC ACC TCA AC-3′ (forward) and 5′-ATG CCG TGT CAA ACT GTG TGT C (reverse); GAPDH: 5′-GCA CCG TCA AGG CTG AGA AC-3′ (forward); and 5′-TGG TGA AGA CGC CAG TGG A-3′ (reverse).

Western blotting

Radioimmunoprecipitation assay lysis buffer (P0013B, Beyotime, Shanghai, China) was used to extract the total protein, followed by sodium dodecyl sulfate polyacrylamide gel electrophoresis (SDS-PAGE) electrophoresis and transfer of the protein to polyvinylidene fluoride (PVDF; IPVH00010, Millipore; Billerica, MA, USA) membranes. SDS-PAGE gels (10%) were prepared, loaded at 30 μg of protein per well, electrophoresed onto PVDF membranes, and blocked in 5% bovine serum albumin for 120 min. Rabbit primary antibodies (Cav-1, 1:1000, 3267, Cell Signaling Technology, Danvers, MA, USA; HuR, 1:1000, ab200342, Abcam, Cambridge, UK; intercellular cell adhesion molecule-1 (ICAM-1), 1:1000, ab109361, Abcam, Cambridge, UK; β-actin, 1:1000, ab8226, Abcam, Cambridge, UK) were added, and the membranes were placed on ice. On the following day, the membranes were washed after the incubation cassette was removed and then re-suspended at room temperature for 30 min. Horseradish peroxidase -conjugated goat-antirabbit immunoglobulin G (IgG) (1:5000, ab6721, Abcam, Cambridge, UK) was added, and the membranes were incubated at room temperature for 120 min. The membrane was washed 3 times with Tris-buffered saline containing Tween-20 (ST673, Beyotime, Shanghai, China) and developed through chemiluminescent detection (ChemiDoc XRS+, Bio-Rad ChemiDoc, California, USA). The relative protein gray values were calculated by normalizing to β-actin protein as a loading reference using Image J (National Institutes of Health, Bethesda, MA, USA).

Enzyme-linked immunosorbent assay (ELISA) analysis and reactive oxygen species (ROS) detection

The levels of IL-6, tumor necrosis factor-α (TNF-α), and IL-1β in the cells and sera were detected using relevant product professional detection ELISA kits (IL-6, PI330, PI326, Beyotime, Shanghai, China; TNF-α, PT518, PT512, Beyotime, Shanghai, China; IL-1β, PI305, PI301, Beyotime, Shanghai, China). The detection was conducted in strict accordance with the instructions. A ROS assay kit (ab113851, Abcam, Cambridge, UK) was used in quantitatively assessing ROS levels in the cell samples. The cells were attached to 96-well culture plates, washed with buffer, and stained with 2′,7′-dichlorodihydrofluorescein diacetate for 45 min at 37°C. The images and fluorescence intensity were captured and measured using a fluorescence microscope (excitation/emission at 485 nm/535 nm; IX73, Olympus, Tokyo, Japan) and ImageJ software (National Institutes of Health, Bethesda, MA, USA). In addition, the ROS levels in the aortic cryostat sections were assessed using the fluorescent probe dihydroethidium (DHE, D23107, Invitrogen, Waltham, MA, United States). The freshly prepared 5 μm-thick sections of mouse aortas were incubated with 5 μM DHE solution in the dark at 37°C for 10 min. The sections were rinsed with PBS

3 times at 4°C for the removal of excess probes. Subsequently, fluorescence imaging was performed using an excitation wavelength of 518 nm and emission wavelength of 606 nm. The resulting fluorescence, which is indicative of ROS levels, was measured and quantified using ImageJ software (National Institutes of Health, Bethesda, MA, USA).

Cell counting kit-8 (CCK-8)

The HUVECs were digested and prepared as cell suspensions, which were then seeded into a 96-well plate at a density of 2 × 10^3 cells/well for 24 h under standard conditions. At 0, 6, 12, or 24 h, each well was treated with CCK-8 reagent (10 µL; CA1210, Solaibio, Beijing, China) and mixed for 2 h. Using a microplate reader (Multiskan FC, Thermo Fisher, Waltham, MA, USA), the absorbance at 450 nm was measured to detect cell viability.

Cell apoptosis

An annexin V- Fluorescein Isothiocyanate (FITC)/propidium iodide (PI) apoptosis detection kit (556547, BD Bioscience, San Jose, CA, USA) was used in cell apoptosis analysis. HUVECs were resuspended with 500 µL of binding buffer, 5 µL of annexin V-FITC, and 5 µL of PI in the dark at 4°C for 15 min. Finally, apoptosis levels were analyzed with a flow cytometry kit (FACSVERSE, BD Bioscience, San Jose, CA, USA) according to the manufacturer's instruction.

RNA immunoprecipitation (RIP) and biotin pull-down

The binding of Cav-1 and HuR was analyzed using a MEGshortscript T7 kit (AM1354, Thermo Fisher, USA) and an EZ-Magna RIP RNA-binding protein immunoprecipitation kit (17-701, Millipore, Billerica, MA, USA). For the RNA immunoprecipitation (RIP) experiment, a buffer containing control IgG-conjugated magnetic beads or HuR antibodies and cell lysates were prepared. Each sample was incubated at 4°C for 12 h. For the biotin pull-down experiment, streptavidin-conjugated beads containing Cav-1 mRNA 3' and 5' UTRs or coding regions were prepared, and cell lysates were added. Each sample was left to stand at 4°C for 3 h. The eluents obtained with the two procedures were respectively analyzed through Western blotting and qPCR.

Vascular oil red O staining

The aorta fixed with 4% paraformaldehyde was cut along the long axis of the blood vessel under a dissection microscope and washed twice with PBS, and the blood vessel was expanded and fixed on a white bottom plate. The aorta was immersed in an Oil Red O staining solution (O8010, Solarbio, Beijing, China) and incubated at 37°C for 1 h. The differentiation of the cells was induced in 75% ethanol until the lipid droplets were orange or bright red and then photographed. The area of lesion positively stained by Oil Red O in the entire aorta or aortic root was evaluated using Image J software (National Institutes of Health, Bethesda, MA, USA).

Statistical analysis

After data collection, statistical analysis was performed using the Statistical Package for the Social Sciences 18.0 software (IBM Corp., USA) and GraphPad Prism 7 (GraphPad Software Inc., San Diego, CA, USA). Whether the data were normally distributed and were determined with the Shapiro–Wilk test, and the homogeneity of variance was verified with Levene's test. Data between groups were analyzed using *t*-tests and one-way analysis of variance. Then, Tukey's *post hoc* test was performed for pairwise comparisons. Data were expressed as mean ± standard deviation, and $P < 0.05$ was considered significant.

RESULTS

P. gingivalis suppressed cell viability and increased Cav-1 expression level

To study the relationship of *P. gingivalis* to the development of AS, we employed the different multiplicity of *P. gingivalis* to infect the HUVECs and then detected cell viability. The CCK-8 assay results showed that *P. gingivalis* infection remarkably decreased the cell viability of the HUVECs, and the inhibitory effect on cell viability was evident at 100 MOI ($P < 0.05$); [Figure 1a]. Moreover, the cell viability of the HUVECs markedly weakened as infection time increased ($P < 0.05$); [Figure 1b]. Given that *P. gingivalis* may contribute to Cav-1 expression,[15] we explored and analyzed HUVECs infected with *P. gingivalis* and examined their Cav-1 levels. The results showed that after infection with *P. gingivalis*, Cav-1 levels showed a significant upward trend with time and concentration ($P < 0.05$); [Figure 1c and d].

Cav-1 triggered *P. gingivalis*-induced oxidative stress, inflammatory responses, and cell apoptosis of HUVECs

To explore whether Cav-1 is involved in *P. gingivalis*-accelerated AS, we exposed the HUVECs to *P. gingivalis* to mimic *P. gingivalis*-accelerated AS *in vitro* and then decreased Cav-1 level with siRNA. Western blotting revealed that HUVECs subjected to *P. gingivalis* showed substantial increase in Cav-1 level, whereas the transfection of si-Cav-1 reduced the *P. gingivalis*-accelerated upregulation of Cav-1 ($P < 0.05$); [Figure 2a]. *P. gingivalis* substantially promoted the production of IL-1β, IL-6, and TNF-α, while silencing of Cav-1 dramatically restored these changes in HUVECs ($P < 0.05$); [Figure 2b-d]. Consistently, the production of ROS induced by *P. gingivalis* was substantially abolished by si-
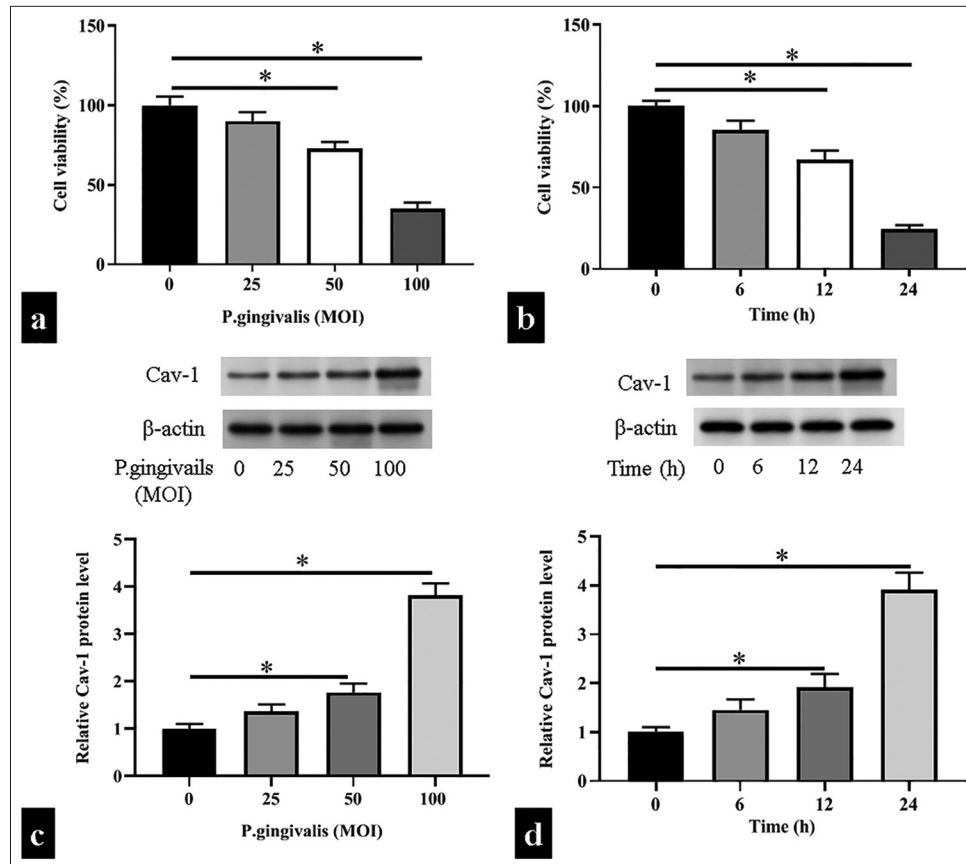
Figure 1: *Porphyromonas gingivalis* suppressed cell viability and increased caveolin 1 (Cav-1) expression level. (a) The viability of human umbilical vein endothelial cells (HUVECs) infected with *P. gingivalis* at different concentrations (multiplicity of infection [MOI]: 0, 25, 50, 100; *n* = 5) with cell counting kit-8 (CCK-8). (b) The viability of HUVECs infected with *P. gingivalis* at a specified MOI (100) for a specified period of time (0, 6, 12, and 24 h) was analyzed with the CCK-8 assay. (c and d) The concentration- and time-dependent expression of Cav-1 in the HUVECs exposed to *P. gingivalis* (n = 3) was analyzed through Western blot analysis. a and c: *$P < 0.05$ versus MOI (0) group; b and d: *$P < 0.05$ versus time (0 h) group.

Cav-1 ($P < 0.05$); [Figure 2e and f]. Flow cytometry showed that silencing of Cav-1 significantly reduced cell apoptosis in the HUVECs infected with *P. gingivalis* ($P < 0.05$); [Figure 2g and h]. The Western blot results further revealed that *P. gingivalis* exposure increased the expression of ICAM-1, whereas Cav-1 silencing in HUVECs reversed this change ($P < 0.05$); [Figure 2i].

HuR directly bound and stabilized Cav-1 mRNA

The 3' UTR of Cav-1 mRNA contains ARE structure.[18] HuR, as an RNA-binding protein, can bind to a variety of 3' UTR mRNAs containing the ARE structure and improve their stability. Therefore, we hypothesized that HuR exerts a regulatory effect on Cav-1 mRNAs. In HUVECs, when HuR expression decreased or increased, Cav-1 protein expression was decreased and increased, respectively ($P < 0.05$), but its mRNA level did not change ($P > 0.05$). This result indicated

that HuR had a regulatory effect on Cav-1 mRNA stability [Figure 3a-c]. Subsequently, we collected cells at different time points after the addition of actinomycin D and detected the remaining amount of Cav-1 mRNA through RT-qPCR. The results showed that the half-life of a Cav-1 mRNA was significantly shortened after si-HuR transfection ($P < 0.05$); [Figure 3d]. Biotin pull-down assay demonstrated that HuR bound with the 3' UTR of the Cav-1 mRNA but not with the 5' UTR or coding region [Figure 3e]. By performing an RIP assay, we found that the HuR antibody pulled down more Cav-1 mRNA than the control IgG antibody ($P < 0.05$); [Figure 3f].

Cav-1 triggered *P. gingivalis*-induced inflammatory responses, oxidative stress, and cell apoptosis of HUVECs by binding to HuR

We further confirmed that Cav-1 activated by HuR affected HUVEC function. The co-overexpression of HuR suppressed
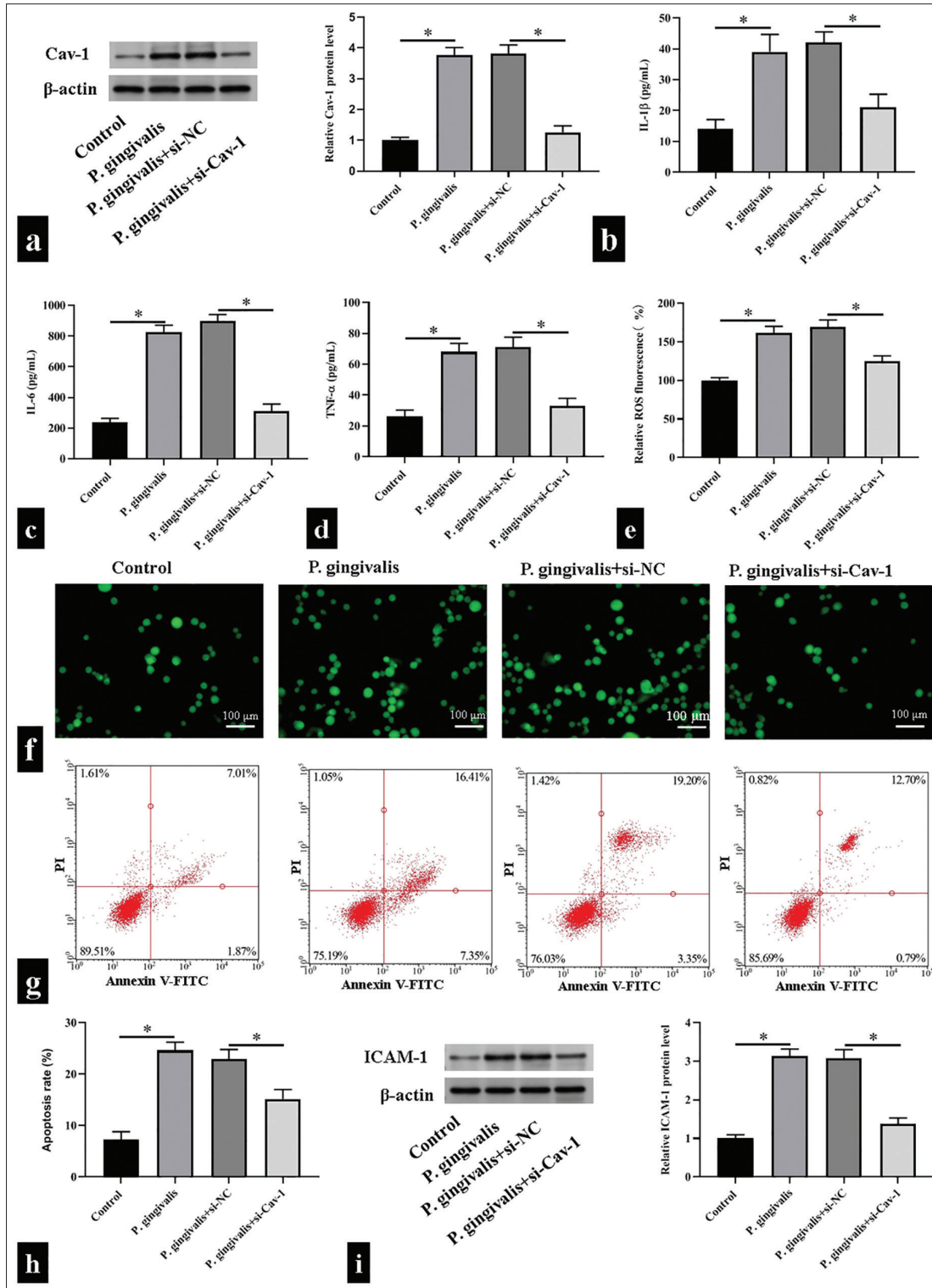
Figure 2: Caveolin 1 (Cav-1) triggered *Porphyromonas gingivalis* (*P. gingivalis*)-induced oxidative stress, inflammatory responses, and cell apoptosis of human umbilical vein endothelial cells. (a) Cav-1 protein levels detected using Western blotting. (b-f) Interleukin (IL)-1β, IL-6, tumor necrosis factor-α, and reactive oxygen species levels detected using enzyme-linked immunosorbent assay kits and 2′,7′-dichlorodihydrofluorescein diacetate fluorescence probe, respectively, scale bar = 100 μm (*n* = 5). (g and h) Detected cell apoptosis levels using flow cytometry (*n* = 3). (i) Detected intercellular cell adhesion molecule-1 (ICAM-1) protein levels using Western blotting. (*n* = 3). si-NC: small interfering RNA negative control, si-Cav-1: small interfering RNA Caveolin 1, V-FITC: V-Fluorescein Isothiocyanate.*$P < 0.05$.
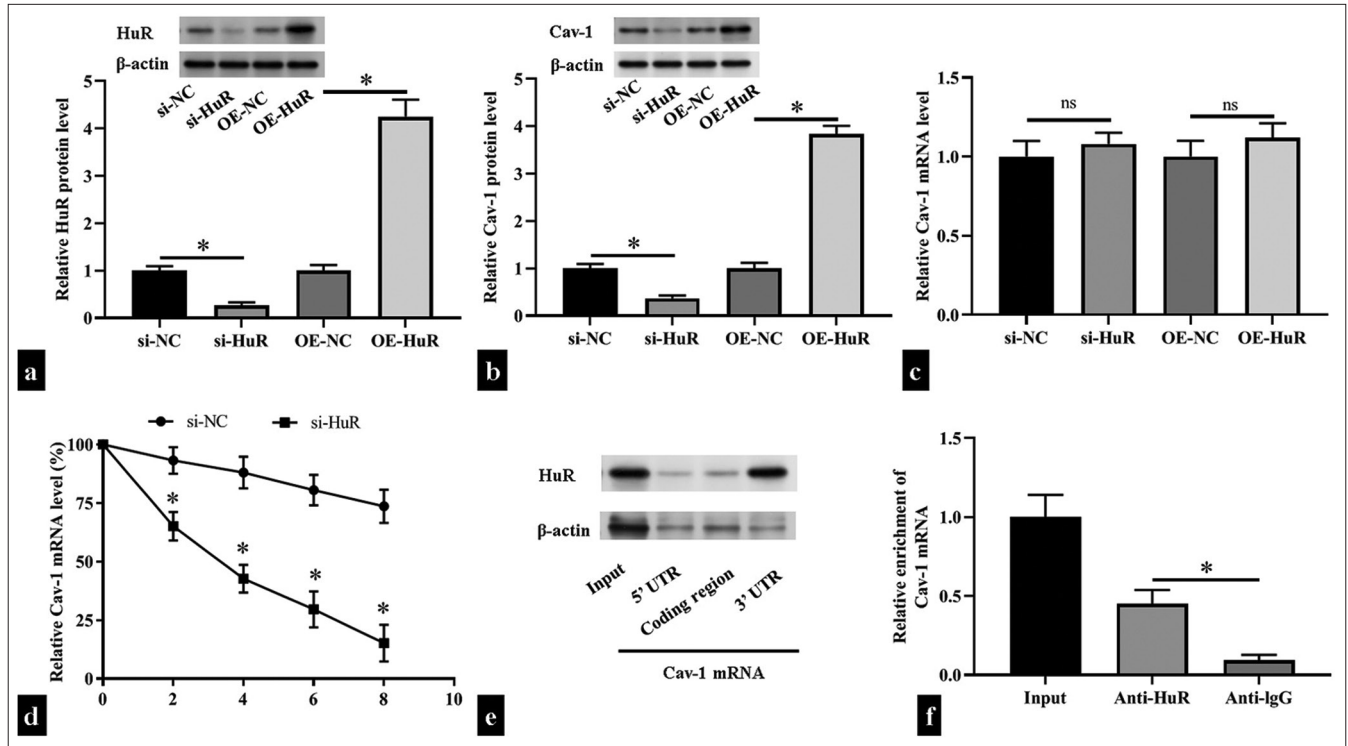
Figure 3: Human antigen R (HuR) directly bound to the caveolin 1 (Cav-1) messenger ribonucleic acid (mRNA) and stabilized it. (a-c) The levels of HuR and Cav-1 protein and mRNA levels after transfection small interfering RNA HuR (si-HuR), HuR overexpression plasmid (OE-HuR), or corresponding negative controls in human umbilical vein endothelial cells (HUVECs) ($n = 3$) were measured through Western blotting and reverse transcription quantitative polymerase chain reaction (RT-qPCR). (d) The levels of Cav-1 in si-HuR- or negative control small interfering RNA -transfected HUVECs were measured through RT-qPCR after actinomycin D treatment ($n = 5$). (e) Biotin pull-down assay detection of the binding between HuR and the 3′ untranslated region (UTR), coding region, and 5' UTR of the Cav-1 mRNA ($n = 3$). (f) RNA immunoprecipitation experiments detection of the binding of HuR to Cav-1 in HUVECs treated with anti-HuR and anti-immunoglobulin G (negative control; $n = 5$). UTR: Untranslated region, si-NC: small interfering RNA negative control, OE-NC: Overexpression plasmid negiative control, ns: no significant. $^{ns}P > 0.05$, $^{*}P < 0.05$.

the inhibitory effects of si-Cav-1 on inflammatory responses and oxidative stress, increasing IL-1β, IL-6, and TNF-α levels and promoting ROS production ($P < 0.05$); [Figure 4a-e]. Simultaneously, Cav-1 inhibition significantly reduced apoptosis; however, the co-overexpression of HuR and si-Cav-1 increased apoptosis ($P < 0.05$); [Figure 4f and g]. In addition, Cav-1 inhibition substantially diminished the protein levels of Cav-1 and ICAM-1, while HuR overexpression enhanced the decrease of Cav-1 and ICAM-1 expression induced by Cav-1 inhibition in HUVEC subjected to *P. gingivalis* ($P < 0.05$); [Figure 4h].

Cav-1 was involved in *P. gingivalis*-induced atherosclerotic plaque formation

To investigate the effect of *P. gingivalis* on AS and the role of Cav-1, we infected the ApoE$^{−/−}$ mice with *P. gingivalis* and injected them with si-Cav-1 through adenovirus infection. We then analyzed plaque formation in the outflow tract of the mouse aorta after *P. gingivalis* infection through Oil Red O staining. The results showed that after *P. gingivalis*

infection, plaque formed in the inner wall of the outflow tract of the aorta, the intimal thickening was evident, and a large amount of lipid was deposited in the plaque. By contrast, *P. gingivalis*-accelerated plaque formation diminished after Cav-1 inhibition ($P < 0.05$); [Figure 5a and b]. Western blotting showed that ApoE$^{−/−}$ mice infected with *P. gingivalis* had increased Cav-1 levels, whereas the ApoE$^{−/−}$ mice treated with si-Cav-1 had significantly decreased Cav-1 levels ($P < 0.05$); [Figure 5c] Moreover, *P. gingivalis* infection with ApoE$^{−/−}$ mice substantially aggravated the IL-6, IL-1β, and TNF-α as well as ROS production, which could be restore after si-Cav-1 treatment ($P < 0.05$); [Figure 5d-h].

DISCUSSION

Periodontal pathogenic microorganisms play an important role in the relationship between chronic periodontitis and cardiovascular diseases. To date, *P. gingivalis*-induced AS, which leads to serious cardiovascular diseases, has been extensively explored. *P. gingivalis* promoting AS plaque formation is considered to be an extremely complex
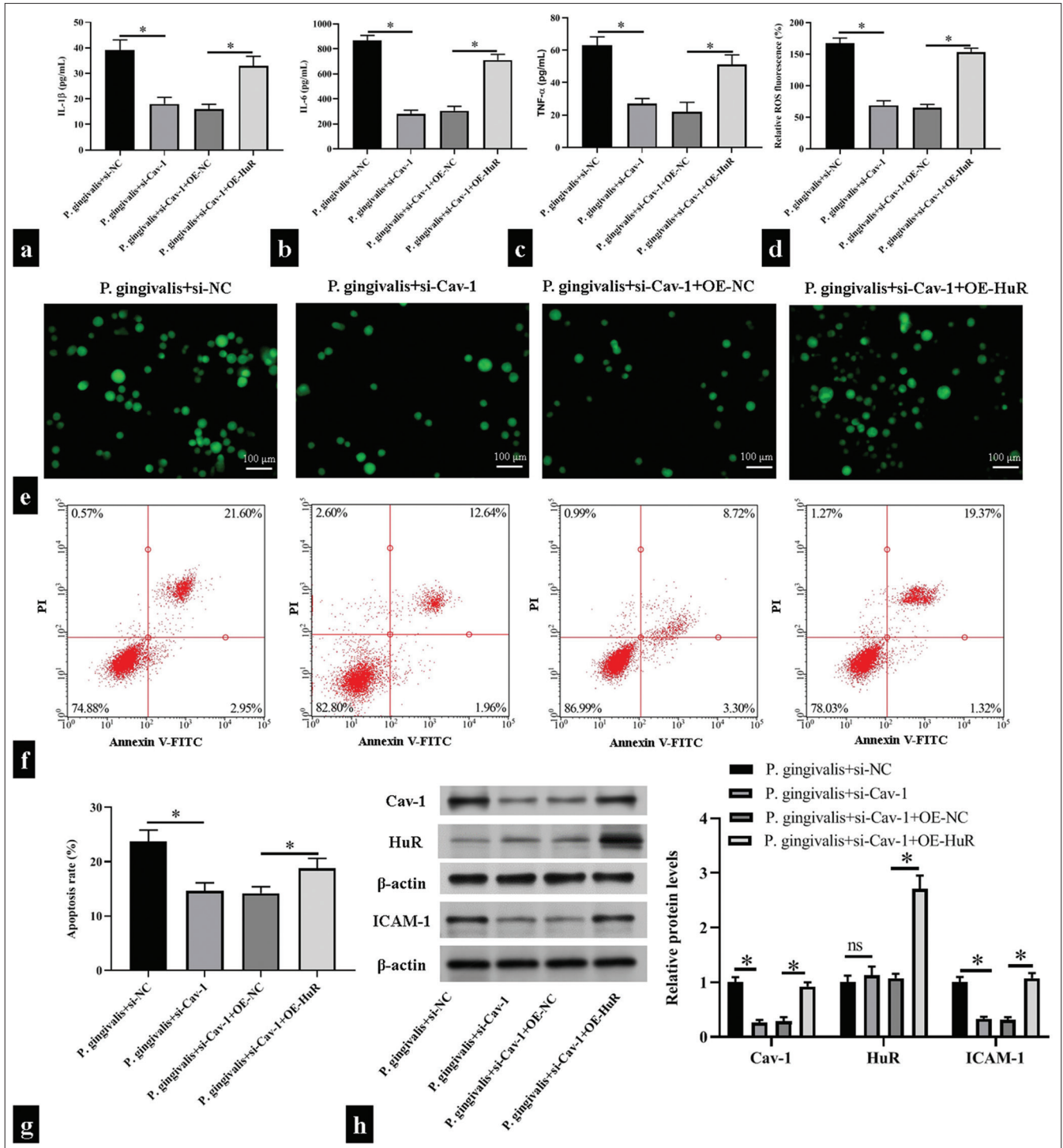
Figure 4: Caveolin 1 (Cav-1) triggered *Porphyromonas gingivalis* (*P. gingivalis*)-induced inflammatory responses, oxidative stress, and cell apoptosis of human umbilical vein endothelial cells (HUVECs) by binding to human antigen R (HuR). HUVECs were transfected with small interfering ribonucleic acid HuR (si-HuR) alone or together with overexpression HuR (OE-HuR) plasmid and then subjected to *P. gingivalis*. (a-e) Enzyme-linked immunosorbent assay kits and 2′,7′-dichlorodihydrofluorescein diacetate fluorescence probe were used in measuring the levels of interleukin (IL)-1β, IL-6, tumor necrosis factor-α, and reactive oxygen species in the supernatant of the HUVECs; Scale bar = 100 μm; (*n* = 5). (f and g) Flow cytometry was used in detecting changes in apoptosis level in the HUVECs (*n* = 5). (h) Changes in Cav-1, HuR, and intercellular cell adhesion molecule-1 (ICAM-1) levels were detected through Western blotting (*n* = 3). si-NC: small interfering RNA negative control, OE-NC: Overexpression plasmid negiative control, V-FITC: V-Fluorescein Isothiocyanate. *$P < 0.05$.
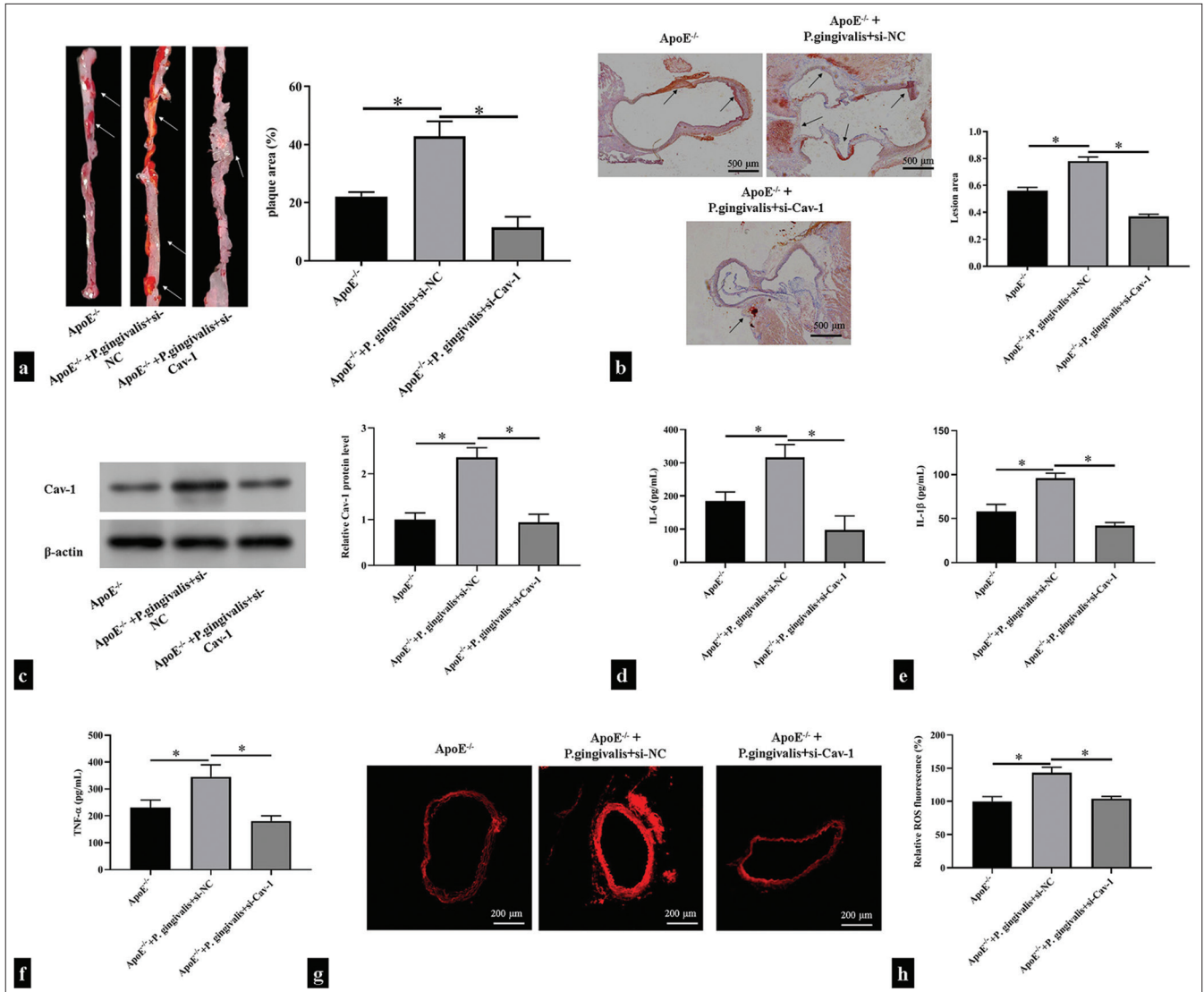
Figure 5: Caveolin 1 (Cav-1) was involved in *Porphyromonas gingivalis*-induced atherosclerotic plaque formation. ApoE$^{-/-}$ mice were injected with si-Cav-1 and then infected with *P. gingivalis*. (a) Oil Red O-stained thoracoabdominal aortas of the ApoE$^{-/-}$ mice (*n* = 5). The white arrow showed areas of atherosclerotic lesions on the surface of the aorta. (b) Oil Red O-stained mouse aortic roots of the ApoE$^{-/-}$ mice (*n* = 5). Scale bar = 500 μm. Magnification is 20x. The black arrow shows areas of atherosclerotic lesions in the aortic root. (c) Western blotting detection of Cav-1 in mouse aortic tissues (*n* = 5). (d-h) Enzyme-linked immunosorbent assay and dihydroethidium fluorescence probe detection of the levels of proinflammatory cytokines and reactive oxygen species in the supernatant of the mouse aortic tissues (*n* = 5). Scale bar = 200 μm. Magnification is 50x. *$P < 0.05$.

pathophysiological process. *P. gingivalis* can adhere to, invade, and survive in arterial endothelial cells and smooth muscle cells.[21] *P. gingivalis* invades endothelial cells, activates the expression of inflammatory factors and adhesion molecules, and promotes the proliferation of smooth muscle cells to accelerate the progression of AS.[19] In addition, *P. gingivalis* infection in AopE$^{-/-}$ mice promotes atherosclerotic plaque formation.[22] However, how *P. gingivalis* affects endothelial cell function remains unclear. *P. gingivalis* can considerably reduce the survival rate of HUVECs, which can contain a large amount of Cav-1. When endothelial cells are infected with *P.*

gingivalis, it can produce inflammatory reactions, increases the production of ROS and inflammatory factors, promotes cell apoptosis, and ultimately disrupts endothelial function.

Cav-1 is highly expressed in endothelial cells and plays an important role in the regulation of cardiovascular and cerebrovascular diseases. In brain microvascular endothelial cells, silencing Cav-1 contributes to brain repair after stroke by promoting the neuronal differentiation of neural stem cells.[23] It is present in endothelial cells as a pro-atherogenic factor. Lack of Cav-1 in macrophages promotes AS, whereas a lack of Cav-1 in endothelial cells prevents

the formation of atherosclerotic lesions.[24] In endothelial cells, the overexpression of Cav-1 inhibits nitric oxide (NO) production, decreasing vascular cell adhesion molecule 1 expression and increasing inflammation, which, in turn, promotes AS.[25] In addition, Cav-1 upregulates lectin-like oxidized low-density lipoprotein (ox-LDL) receptor 1, which is the receptor of ox-LDL, through the nuclear factor-kappa-B signaling pathway, which increases the accumulation and uptake of ox-LDL in endothelial cells and accelerates AS development.[26,27] Interestingly, *P. gingivalis* infection enhances the formation of caveolae on the endothelial cell membrane surface and the expression of Cav-1 in cells.[15] These results suggest that Cav-1 is involved in AS development induced by *P. gingivalis*. Here, we observed that *P. gingivalis* infection increased Cav-1 expression, while Cav-1 deficiency ameliorated *P. gingivalis*-induced oxidative stress, inflammatory response, and cell apoptosis and inhibited AS plaque formation.

The diversity of HuR downstream target genes determines the breadth and complexity of HuR functions. Given that HuR can regulate the mRNA expression of angiotensin receptor, inducible NO synthase, cyclooxygenase-2, TNF-α, and other genes, HuR also plays an important role in a variety of cardiovascular diseases.[28,29] In addition, HuR level increases in a variety of vascular diseases, including intimal hyperplasia, AS, graft vascular sclerosis, and fibromuscular dysplasia.[30] HuR contributes to aortic plaque formation in ApoE$^{-/-}$ mice by binding to TNF-α, IL-1β, and IL-6 mRNAs, increasing their stability, and promoting inflammatory responses and apoptosis in HUVECs.[31] In *P. gingivalis*-induced periodontitis model mice, HuR expression was enhanced in the epithelial and connective tissues of the mice, enhancing mRNA stability and IL-6 expression but exacerbating inflammatory responses.[32] These results suggest that when cells are infected with *P. gingivalis*, HuR can be activated, which promotes the development of AS. When HUVECs were infected, HuR was activated. Furthermore, HuR bound to the 3′ UTR of Cav-1 mRNA and increased the mRNA stability of Cav-1, thereby increasing the protein expression level. In *P. gingivalis*-infected HUVECs, HuR overexpression basically restored oxidative stress, inflammatory response, and apoptosis caused by Cav-1 knockdown, indicating that HuR mediates the process by which Cav-1 induces *P. gingivalis* and accelerates AS.

SUMMARY

The role of Cav-1 in AS lesions caused by *P. gingivalis* was demonstrated for the 1st time through animal and cell experiments. *P. gingivalis* upregulated the expression of Cav-1, whereas HuR enhanced the stability and expression of Cav-1, which aggravates oxidative stress,

inflammation, and apoptosis induced by *P. gingivalis*. Thus, *P. gingivalis* accelerated AS plaque formation. This study offers valuable insights into the role of the immune mechanism of infection in periodontitis and coronary heart diseases.

AVAILABILITY OF DATA AND MATERIALS

The datasets used during the present study are available from the corresponding author on reasonable request.

ABBREVIATIONS

AS – Atherosclerosis
P. gingivalis – *Porphyromonas gingivalis*
Cav-1 – Caveolin 1
HuR – Human antigen R
HUVECs – Human umbilical vein endothelial cells
MOI – Multiplicity of infection
ICAM-1 – Intercellular cell adhesion molecule-1
ROS – Reactive oxygen species
RNA – Ribonucleic acid
VEGF – Vascular endothelial growth factor
AREs – Adenylate uridine–rich elements
UTRs – Untranslated regions
PBS – Phosphate-buffered saline
siRNA – Small interfering RNA
ATCC – American type culture collection
FBS – Fetal bovine serum
RT-qPCR – RNA stability and reverse transcription quantitative polymerase chain reaction
RIPA – Radioimmunoprecipitation assay
SDS-PAGE – Sodium dodecyl sulfate polyacrylamide gel electrophoresis
PVDF – Polyvinylidene fluoride
ELISA – Enzyme-linked immunosorbent assay
TNF-α – Tumor necrosis factor-α
IL-1β – Interleukin-1β
IL-6 – Interleukin-6
DHE – Dihydroethidium
CCK-8 – Cell counting kit-8
PI – Propidium iodide
RIP – RNA immunoprecipitation
SD – Standard deviation
ox-LDL – Oxidized low-density lipoprotein
NF-κB – Nuclear factor-kappa-B

AUTHOR CONTRIBUTIONS

FM: Conceptualization, Formal analysis; YYL: Conceptualization, Methodology, Investigation; YFG: Methodology, Formal analysis, Data Curation; YXM: Conceptualization, Formal analysis, Data curation; YZ: Data Curation, Supervision; BBJ: Investigation, Methodology, Writing-Original Draft.

ETHICS APPROVAL AND CONSENT TO PARTICIPATE

This study was approved by the Animal Experiment Ethics Committee of the Second People's Hospital of Lanzhou City (LZSKQYY-LL-ZD-2024-01). This article does not involve patients, so informed consent is not required.

ACKNOWLEDGMENT

FUNDING

CONFLICT OF INTEREST

The authors declare no conflict of interest.

EDITORIAL/PEER REVIEW

To ensure the integrity and highest quality of CytoJournal publications, the review process of this manuscript was conducted under a **double-blind model** (authors are blinded for reviewers and vice versa) through an automatic online system.

REFERENCES

1. Sanz M, Marco Del Castillo A, Jepsen S, Gonzalez-Juanatey JR, D'Aiuto F, Bouchard P, *et al*. Periodontitis and cardiovascular diseases: Consensus report. J Clin Periodontol 2020;47:268-88.
2. Schenkein HA, Papapanou PN, Genco R, Sanz M. Mechanisms underlying the association between periodontitis and atherosclerotic disease. Periodontol 2000 2020;83:90-106.
3. Vázquez-Reza M, López-Dequidt I, Ouro A, Iglesias-Rey R, Campos F, Blanco J, *et al*. Periodontitis is associated with subclinical cerebral and carotid atherosclerosis in hypertensive patients: A cross-sectional study. Clin Oral Investig 2023;27:3489-98.
4. Yakob M, Meurman JH, Jogestrand T, Nowak J, Söder PÖ, Söder B. C-reactive protein in relation to early atherosclerosis and periodontitis. Clin Oral Investig 2012;16:259-65.
5. Hanaoka Y, Soejima H, Yasuda O, Nakayama H, Nagata M, Matsuo K, *et al*. Level of serum antibody against a periodontal pathogen is associated with atherosclerosis and hypertension. Hypertens Res 2013;36:829-33.
6. Fiehn NE, Larsen T, Christiansen N, Holmstrup P, Schroeder TV. Identification of periodontal pathogens in atherosclerotic vessels. J Periodontol 2005;76:731-6.
7. Rath SK, Mukherjee M, Kaushik R, Sen S, Kumar M. Periodontal pathogens in atheromatous plaque. Indian J Pathol Microbiol 2014;57:259-64.
8. Arjunan P, Swaminathan R, Yuan J, Al-Shabrawey M, Espinosa-Heidmann DG, Nussbaum J, *et al*. Invasion of human retinal pigment epithelial cells by *Porphyromonas gingivalis* leading to vacuolar/cytosolic localization and autophagy dysfunction *in-vitro*. Sci Rep 2020;10:7468.
9. Wang M, Shakhatreh MA, James D, Liang S, Nishiyama S, Yoshimura F, *et al*. Fimbrial proteins of *Porphyromonas gingivalis* mediate *in vivo* virulence and exploit TLR2 and complement receptor 3 to persist in macrophages. J Immunol 2007;179:2349-58.
10. Liu G, Deng J, Zhang Q, Song W, Chen S, Lou X, *et al*. *Porphyromonas gingivalis* Lipopolysaccharide stimulation of vascular smooth muscle cells activates proliferation and calcification. J Periodontol 2016;87:828-36.
11. Wu Q, Li Z, Zhang Y, Luo K, Xu X, Li J, *et al*. Cyclic di-AMP rescues *Porphyromonas gingivalis*-aggravated atherosclerosis. J Dent Res 2023;102:785-94.
12. Cohen AW, Hnasko R, Schubert W, Lisanti MP. Role of caveolae and caveolins in health and disease. Physiol Rev 2004;84:1341-79.
13. Shao S, Qin T, Qian W, Li X, Li W, Han L, *et al*. Cav-1 ablation in pancreatic stellate cells promotes pancreatic cancer growth through Nrf2-induced SHH signaling. Oxid Med Cell Longev 2020;2020:1868764.
14. Shetti AU, Ramakrishnan A, Romanova L, Li W, Vo K, Volety I, *et al*. Reduced endothelial caveolin-1 underlies deficits in brain insulin signalling in type 2 diabetes. Brain 2023;146:3014-28.
15. Lei S, Li J, Yu J, Li F, Pan Y, Chen X, *et al*. *Porphyromonas gingivalis* bacteremia increases the permeability of the blood-brain barrier via the Mfsd2a/Caveolin-1 mediated transcytosis pathway. Int J Oral Sci 2023;15:3.
16. Tamai R, Asai Y, Ogawa T. Requirement for intercellular adhesion molecule 1 and caveolae in invasion of human oral epithelial cells by *Porphyromonas gingivalis*. Infect Immun 2005;73:6290-8.
17. López de Silanes I, Zhan M, Lal A, Yang X, Gorospe M. Identification of a target RNA motif for RNA-binding protein HuR. Proc Natl Acad Sci U S A 2004;101:2987-92.
18. Cao S, Xiao L, Wang J, Chen G, Liu Y. The RNA-binding protein HuR regulates intestinal epithelial restitution by modulating Caveolin-1 gene expression. Biochem J 2021;478:247-60.
19. Xie M, Tang Q, Nie J, Zhang C, Zhou X, Yu S, *et al*. BMAL1-downregulation aggravates *Porphyromonas gingivalis*-induced atherosclerosis by encouraging oxidative stress. Circ Res 2020;126:e15-29.
20. Zhu Y, Yang X, Zhou J, Chen L, Zuo P, Chen L, *et al*. miR-340-5p mediates cardiomyocyte oxidative stress in diabetes-induced cardiac dysfunction by targeting Mcl-1. Oxid Med Cell Longev 2022;2022:3182931.
21. Dorn BR, Dunn WA Jr., Progulske-Fox A. Invasion of human coronary artery cells by periodontal pathogens. Infect Immun 1999;67:5792-8.
22. Gibson FC 3rd, Hong C, Chou HH, Yumoto H, Chen J, Lien E, *et al*. Innate immune recognition of invasive bacteria accelerates atherosclerosis in apolipoprotein E-deficient mice.

Circulation 2004;109:2801-6.

23. Li Y, Zhao Y, Gao C, Wu M, So KF, Tong Y, *et al.* Caveolin-1 derived from brain microvascular endothelial cells inhibits neuronal differentiation of neural stem/progenitor cells *in vivo* and *in vitro*. Neuroscience 2020;448:172-90.

24. Pavlides S, Gutierrez-Pajares JL, Katiyar S, Jasmin JF, Mercier I, Walters R, *et al.* Caveolin-1 regulates the anti-atherogenic properties of macrophages. Cell Tissue Res 2014;358:821-31.

25. Fernández-Hernando C, Yu J, Dávalos A, Prendergast J, Sessa WC. Endothelial-specific overexpression of caveolin-1 accelerates atherosclerosis in apolipoprotein E-deficient mice. Am J Pathol 2010;177:998-1003.

26. Sun SW, Zu XY, Tuo QH, Chen LX, Lei XY, Li K, *et al.* Caveolae and caveolin-1 mediate endocytosis and transcytosis of oxidized low density lipoprotein in endothelial cells. Acta Pharmacol Sin 2010;31:1336-42.

27. Bian F, Cui J, Zheng T, Jin S. Reactive oxygen species mediate angiotensin II-induced transcytosis of low-density lipoprotein across endothelial cells. Int J Mol Med 2017;39:629-35.

28. Linker K, Pautz A, Fechir M, Hubrich T, Greeve J, Kleinert H. Involvement of KSRP in the post-transcriptional regulation of human iNOS expression-complex interplay of KSRP with TTP and HuR. Nucleic Acids Res 2005;33:4813-27.

29. Aguado A, Rodríguez C, Martínez-Revelles S, Avendaño MS, Zhenyukh O, Orriols M, *et al.* HuR mediates the synergistic effects of angiotensin II and IL-1β on vascular COX-2 expression and cell migration. Br J Pharmacol 2015;172:3028-42.

30. Pullmann R Jr., Juhaszova M, López de Silanes I, Kawai T, Mazan-Mamczarz K, Halushka MK, *et al.* Enhanced proliferation of cultured human vascular smooth muscle cells linked to increased function of RNA-binding protein HuR. J Biol Chem 2005;280:22819-26.

31. Bai J, Liu J, Fu Z, Feng Y, Wang B, Wu W, *et al.* Silencing lncRNA AK136714 reduces endothelial cell damage and inhibits atherosclerosis. Aging (Albany NY) 2021;13:14159-69.

32. Ouhara K, Munenaga S, Kajiya M, Takeda K, Matsuda S, Sato Y, *et al.* The induced RNA-binding protein, HuR, targets 3'-UTR region of IL-6 mRNA and enhances its stabilization in periodontitis. Clin Exp Immunol 2018;192:325-36.

NextGen CelBloking™ Kits

Frustrated with your cell blocks?
We have a better solution!

Nano

Nano NextGen CelBloking™

Cell block kit to process single scattered cell specimens and tissue fragments of **any cellularity**.

PATENT PENDING

Pack #1

Pack #2

Micro

Micro NextGen CelBloking™

For cellular specimens (more than 1 ml concentrated specimen with Tissuecrit more than 50%)

PATENT PENDING

Pack #1

Pack #2

www.AVBioInnovation.com